Supplementary Materials (SM) for:

Alloy-oxide interfacial ensemble effect of multilayer core-shell nanomotor for hydrogen generation from ammonia borane

Shuyan Guan, [a, b #] Yong Guo,[a,#] Huanhuan Zhang,[a, b] Xianyun Liu,[a,b] Yanping Fan[a,b]*, and Baozhong Liu, [a,b,]*

[a] College of Chemistry and Chemical Engineering, Henan Polytechnic University, 2001 Century Avenue, Jiaozuo 454000, P.R. China.

[b] State Collaborative Innovation Center of Coal Work Safety and Clean-efficiency Utilization, Jiaozuo 454003, PR China

[#] These authors contributed equally to this work.

* Corresponding Author. E-mail: fanyanping@hpu.edu.cn (Y. P. Fan), and HPUliuking@163.com (B. Z. Liu).

Table of Contents

Total number of Pages: 18

Total number of Figures: 11

Total number of Tables: 2

Experimental Section

1. Materials: All chemical reagents were purchased from commercial suppliers and no further purification was required before use. The materials used in this study were AB (NH_3BH_3, 97%, Aladdin), cobalt nitrate hexahydrate ($Co(NO_3)_2 \cdot 6H_2O$, Shanghai Macklin Biochemical Co., Ltd., AR, 99%), Copper nitrate hydrate ($Cu(NO_3)_2 \cdot 5H_2O$, AR, 99%, Shanghai Macklin Biochemical), p-Phthalic acid (PTA) (99%, AR, Shanghai Macklin Biochemical). Anhydrous methanol and ethanol were purchased from Tianjin Concord Co., Ltd.

2.Characterization. The powder X-ray diffraction (XRD) analysis is carried out using a Rigaku TTR3 X-ray powder diffractometer with Cu K_α radiation (λ=1.5406 Å). The surface morphology of the catalyst is studied using a Merlin Compact scanning electron microscope (SEM). Transmission electron microscope (TEM) and high-resolution transmission electron microscope (HRTEM) images are obtained on a FEI Tecnai G^2 F20 high-resolution transmission electron microscope operating at 200 kV. Thermal gravimetric analysis (TGA) is carried out on the STA 409 PC/PG (NETZSCH Germany) at 800 ℃ with a heating rate of 10 ℃ min^{-1}. The samples of CoCu-MOF and CoO@CoCu-C are studied using a Varian 720 inductively coupled plasma-optical emission spectrometers (ICP-OES). X-ray photoelectron spectroscopy (XPS) measurement is performed with PHI 5000 Versa Probe.

3.The Density functional theory (DFT) simulations calculation method. The present first principle DFT calculations are performed with the projector augmented wave (PAW) method. [S1, S2] The exchange-functional is treated using the generalized gradient approximation (GGA) of Perdew-Burke-Ernzerhof (PBE) [S3] functional. The cut-off energy of the plane-wave basis is set at 450 eV for optimize calculations of atoms and cell optimization. The vacuum spacing in a direction perpendicular to the plane of the catalyst is 15 Å. The Brillouin zone integration is performed using 3×3×1 Monkhorst-Pack k-point sampling for structure. The self-consistent calculations apply a convergence energy threshold of 10^{-6} eV. The equilibrium lattice constants are optimized with maximum stress on each atom within 0.05 eV/Å. The Hubbard U (DFT+U) corrections for 3d transition metal by setting according to the literature.

Finally, the free energies are obtained by $G=E_{total}+E_{ZPE}-TS$, where E_{total}, E_{ZPE}, and TS is the ground-state energy, zero-point energies, and entropy terms, respectively.

Supplementary Figures

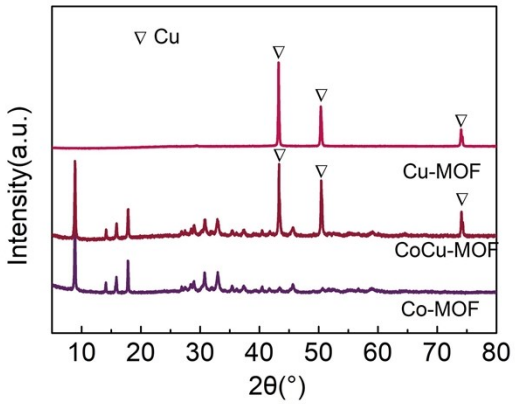

Fig. S1. The XRD of Co-MOF, CoCu-MOF and Cu-MOF.

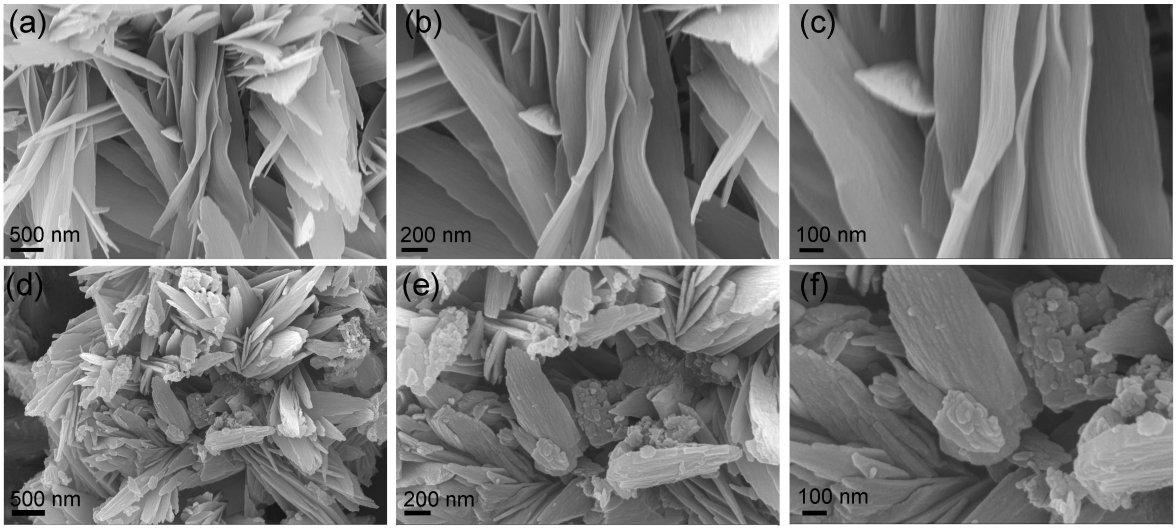

Fig. S2. (a-c) SEM images of Co-MOF, (d-f) and SEM images of CoCu-MOF

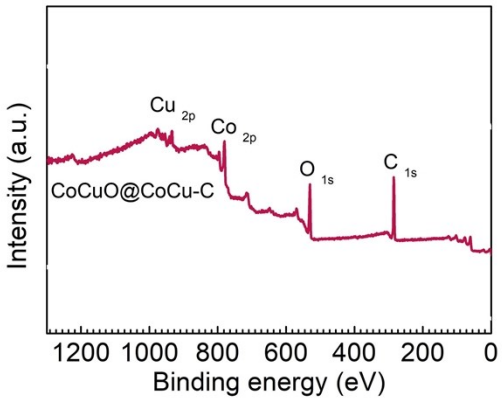

Fig. S3. The total X-ray spectrum of CoCuO@CoCu-C.

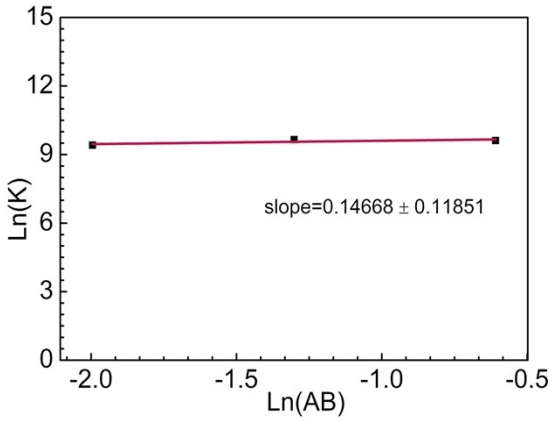

Fig. S4. Logarithmic plot of AB concentration and rate constant.

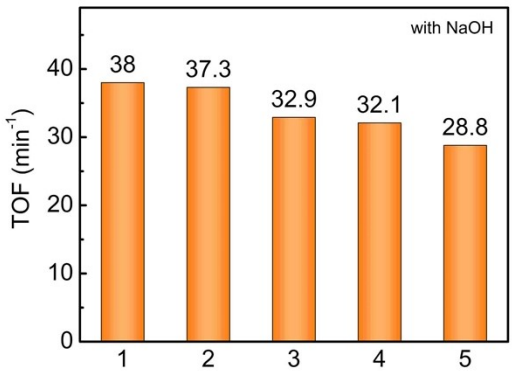

Fig S5. TOF of CoCuO@CoCu-C in cyclic stability test.

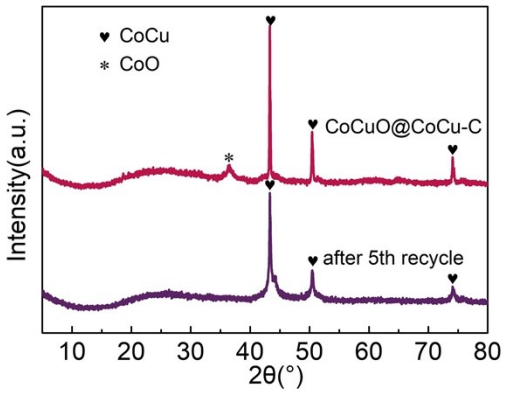

Fig S6. The XRD of CoCuO@CoCu-C before recycle and after 5th recycle.

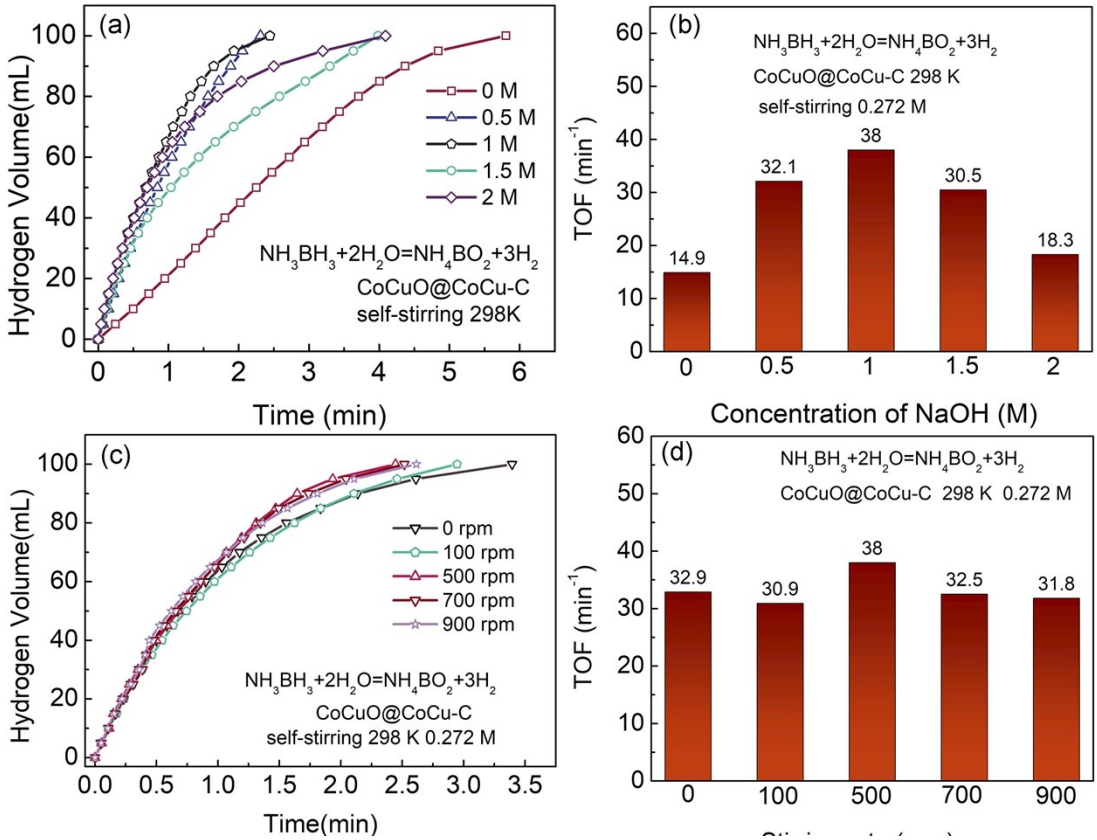

Fig. S7. Hydrogen generation catalyzed by (a) different concentration of NaOH, (b) corresponding TOF, (c) different rotate speed and (d) corresponding TOF of CoCuO@CoCu-C at 298 K.

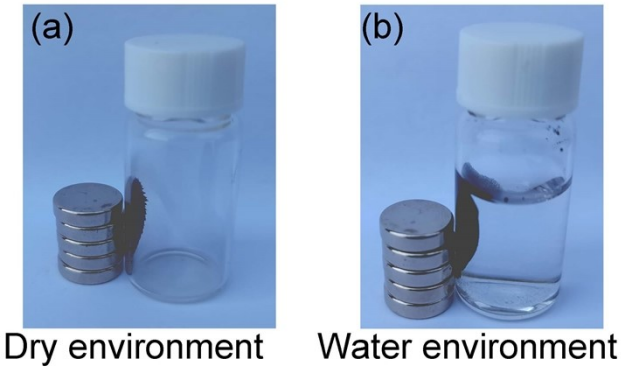

Fig. S8. View of the magnetism of CoCuO@CoCu-C in the (a) dry environment and (b) water environment.

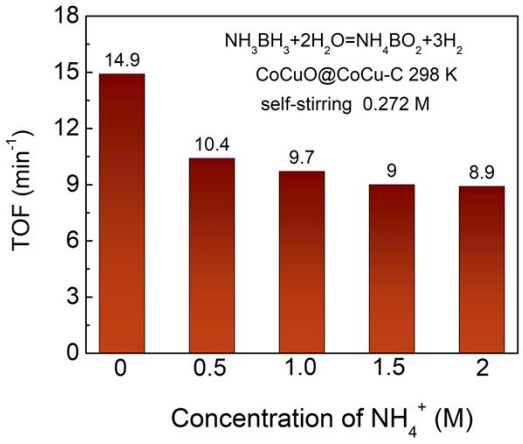

Fig. S9. The TOF at different concentration of NH_4^+.

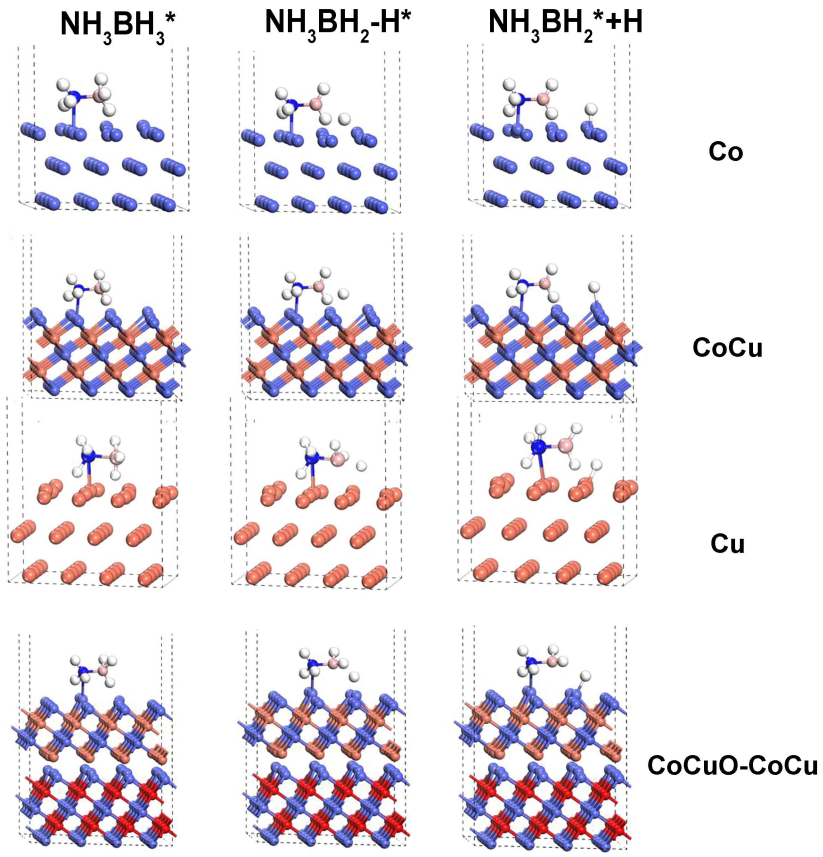

Fig S10. The optimized 3D models of H_2O on the surface of Co, CoCu, Cu, and CoCuO-CoCuO. Co, Cu, B, N, O and H are represented as wathet, win red, blue, pink, red and white sphere, respectively.

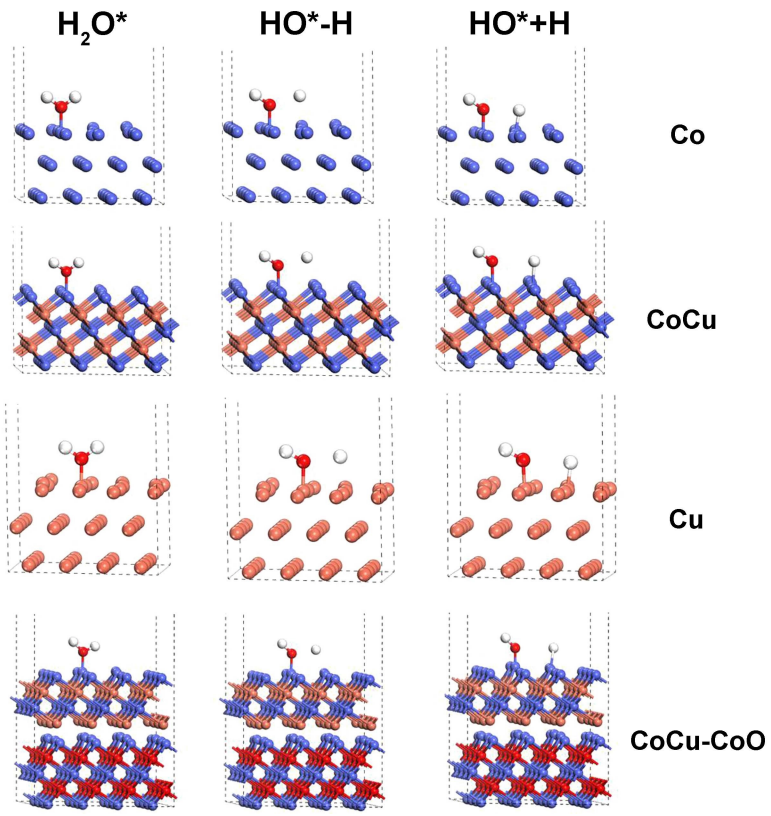

Fig S11. The optimized 3D models of H_2O on the surface of Co, CoCu, Cu, and CoCuO-CoCuO. Co, Cu, B, N, O and H are represented as wathet, win red, blue, pink, red and white sphere, respectively.

Supplementary Tables

Table S1. The ratios of Cu/Co for CoCu-MOF and CoO@CoCu-C tested by ICP-AES.

Raw material molar ratio (Cu:Co) ratio	1:1	1:1
Cu:Co(mol%)	22.65:21.71	34.09:35.72
Samples	CoCu-MOF	CoO@CoCu-C

Table S2. Catalytic activities and E_a values of Co-based catalysts used for the hydrolytic dehydrogenation of AB.

Catalyst	Temp.(K)	TOF (min^{-1})	E_a (kJ/mol)	Cyclic test	Ref
CoO@CoCu-C	**298**	**37.56 (mol $_{hydrogen}$ mol $_{Co}^{-1}$)**	**27.6**	**75.8% /5**	**this work**
CoCu/Ni	298	30.5 (mol $_{hydrogen}$ mol $_{cat}^{-1}$)	/	/	S4
CoP@HPC-500	303	27.7 (mol $_{hydrogen}$ mol $_{Co}^{-1}$)	42.5	8 times	S5
$Cu_6Fe_{0.8}Co_{3.2}$@MIL-	298	23.2 (mol $_{hydrogen}$ mol $_{cat}^{-1}$)	37.1	7 times	S6
Co-Co_3O_4/CDs	298	17.93 (mol $_{hydrogen}$ mol $_{Co}^{-1}$)	/	50%/5	S7
$Co_{0.9}W_{0.1}$/RGO	298	16.4 (mol $_{hydrogen}$ mol $_{cat}^{-1}$)	30.7	5 times	S8
CoNPs/Mxene	298	12.5 (mol $_{hydrogen}$ mol $_{cat}^{-1}$)	/	6 times	S9
$Cu_{0.4}Co_{0.6}$/BNNFs	298	8.42 (mol $_{hydrogen}$ mol $_{cat}^{-1}$)	21.8	55%/5	S10
Co/NPCNW	298	7.29 (mol $_{hydrogen}$ mol $_{Co}^{-1}$)	25.4	90%/10	S11
Co@N-C-700	298	5.6 (mol $_{hydrogen}$ mol $_{cat}^{-1}$)	21.8	97%/10	S12
Co/Al_2O_3	298	4.98 (mol $_{hydrogen}$ mol $_{Co}^{-1}$)	/	/	S13

REFERENCES

S1 J.P. Perdew, K. Burke, M. Ernzerhof, Generalized gradient approximation made simple. Phys. Rev. Lett. 78 (1997) 1396.

S2 G. Kresse, D. Joubert, From ultrasoft pseudopotentials to the projector augmented wave method. Phys. Rev. B 59 (1999) 1758.

S3 J.P. Perdew, K. Burke, M. Ernzerhof, Generalized gradient approximation made simple, Phy. Rev. Lett. 77 (1996) 3865.

S4 I.Y. Liao, F. Lv, Y.F. Feng, S.D. Zhong, X.X. Wu, X.B. Zhang, J.J. Li, H. Li, Electromagnetic-field-assisted synthesis of Ni foam film-supported CoCu alloy microspheres composed of nanosheets: a high performance catalyst for the hydrolysis of ammonia borane. Catal. Commun. 122 (2019) 16-19.

S5 X.C. Ma, Y.Y. He, D.X. Zhang, M.J. Chen, S.C. Ke, Y.X. Yin, G.G. Chang, Cobalt-based MOF-derived CoP/hierarchical porous carbon (HPC) composites as robust catalyst for efficient dehydrogenation of ammonia-borane. ChemistrySelect 5 (2020) 2190-2196.

S6 Y. Li, S.F. Li, Low-cost CuFeCo@MIL-101 as an efficient catalyst for catalytic hydrolysis of ammonia borane. Int. J. Hydrogen Energy. 45 (2020) 10433-10441.

S7 H. Wu, B. J. Li, B. Z. Liu, S. Y. Lu, Interface electron collaborative migration of Co-Co_3O_4/carbon dots: Boosting the hydrolytic dehydrogenation of ammonia borane. J. Energy Chem. 48 (2020) 43-53.

S8 X.G. Du, Y.P. Tai, H.Y. Liu, J. Zhang, One-step synthesis of reduced graphene oxide supported CoW nanoparticles as efficient catalysts for hydrogen generation from NH_3BH_3. React. Kinet. Mech. Catal. 125 (2018) 171-181.

S9 T. Liu, Q.T. Wang, Y.H. Sun, M. Zhao, Facile synthesis of monodispersed Co nanoparticles on titanium carbides for hydrolysis of ammonia borane at mild temperature. J. Nanosci. Nanotechnol. 19 (2019) 7392-7397.

S10 X. Yang, Q.L. Li, L.L. Li, J. Li, X.J. Yang, C. Yu, Z.Y. Liu, CuCo binary metal nanoparticles supported on boron nitride nanofibers as highly efficient catalysts for hydrogen generation from hydrolysis of ammonia borane. J. Power Sources. 431 (2019) 135-143.

S11 L.M. Zhou, J. Meng, P. Li, Z.L. Tao, J. Chen, Ultrasmall cobalt nanoparticles supported on nitrogen-doped porous carbon nanowires for hydrogen evolution from ammonia borane. Mater. Horiz. 4 (2017) 268-273.

S12 X. H, Y. Wang, F.Y. Zhao, Z.L. Cheng, J. Tao, Cobalt nanoparticles embedded in porous N-doped carbon as long-life catalysts for hydrolysis of ammonia borane. Catal. Sci. Technol. 6 (2016) 3443-3448.

S13 B.B. Ismail, Y. Mehmet, B. Ahmet, C. Metin, S.K. Gulsah, Z. Mehmet, K. Murat, A. Murat, D. Feyyaz, B. Akın, Cobalt nanoparticles supported on alumina nanofibers (Co/Al_2O_3): Cost effective catalytic system for the hydrolysis of methylamine borane. Int. J. Hydrogen Energy. 44 (2019) 28441-28450.